

1 **Impact of Controlled Vacuum Induced Surface Freezing** 2 **on the Freeze Drying of Human Plasma**

3

4 Andrea Arsiccio¹, Paul Matejtschuk², Ernest Ezeajughi², Andrew Riches-Duit⁴, Anwen
5 Bullen^{3,5}, Kiran Malik², Sanj Raut⁴ & Roberto Pisano¹.

6 1. Department of Applied Science and Technology, Politecnico di Torino, 24 corso
7 Duca degli Abruzzi, Torino, 10129 Italy.

8 2. Standardisation Science & 3. Imaging Section, Analytical & Biological Sciences
9 Division & 4. Biotherapeutics Division, National Institute for Biological Standards &
10 Control (NIBSC), Blanche Lane, South Mimms, Potters Bar, Hertfordshire, United
11 Kingdom , EN6 3QG.

12 5. UCL Ear Institute, Gray's Inn Road, London, UK, WC1X 8EE

13

14 Email address of corresponding author : Paul.Matejtschuk@nibsc.org

15

16

17 **ABSTRACT**

18 During the freezing step of a typical freeze drying process, the temperature at which nucleation is induced is
19 generally stochastically distributed, resulting in undesired within-batch heterogeneity. Controlled nucleation
20 techniques have been developed to address this problem; these make it possible to trigger the formation of
21 ice crystals at the same time and temperature in all the batch. Here, the controlled nucleation technique
22 known as vacuum induced surface freezing is compared to spontaneous freezing for the freeze drying of
23 human plasma, a highly concentrated system commonly stored in a dried state. The potency of Factor VIII
24 (FVIII), a sensitive, labile protein present in plasma, and the reconstitution time of the dried cakes are
25 evaluated immediately after freeze drying, and after 1, 3, 6 or 9 months storage at different degradation
26 temperatures. We show that the application of controlled nucleation significantly reduces the reconstitution
27 time and in addition helps to improve FVIII stability.

28
29 **KEYWORDS:** freeze drying, controlled nucleation, plasma, biological activity

30
31 **ABBREVIATIONS:** VISF: Vacuum Induced Surface Freezing

32
33 **1. INTRODUCTION**

34 The freeze-drying process is widely used for preserving labile products in the pharmaceutical industry, by
35 removal of water at low temperature to increase shelf life, without significantly affecting the therapeutic
36 properties of the active ingredients (Fissore, 2019; Franks and Auffret, 2007; Rey and May, 2010; Ward and
37 Matejtschuk, 2019). During freeze drying, the product is first frozen, and water is subsequently removed by
38 sublimation during primary drying and desorption during secondary drying. The two drying phases are
39 performed at low pressure, the first typically at sub-zero temperature, so as to minimize possible degradation
40 stresses.

41 In the field of pharmaceutical freeze drying, where often many thousands of vials or ampoules are
42 processed in a single cycle, the problem of potential heterogeneity within each batch is a major concern.
43 Much of this heterogeneity is related to the freezing step, and specifically to the uncontrolled, random
44 distribution of nucleation temperatures within the batch. The nucleation temperature determines the
45 morphology of the final product, with a high nucleation temperature resulting in larger ice crystals (Searles et
46 al., 2001). In turn, the ice crystal size corresponds to the pore size of the dried product, provided that no

47 collapse occurs, and has therefore an impact on process efficiency (Capozzi and Pisano, 2018; Hottot et al.,
48 2007; Kasper and Friess, 2011; Pikal et al., 2002). For instance, a large pore size speeds up the removal of
49 water by sublimation, reducing the primary drying time, but results in a slow desorption rate during secondary
50 drying (Oddone et al., 2016; Oddone et al., 2017).

51 A small ice crystal size also results in the formation of a large ice-water interface, where amphiphilic
52 molecules, such as proteins, could get adsorbed and unfold because of their interaction with the surface
53 (Strambini and Gabellieri, 1996). This surface-induced stress adds up to the risk of cold denaturation
54 (Franks, 1995; Privalov, 1990) that may occur because of the low temperature used during freezing, and it
55 has been shown that for many proteins it actually is the main source of protein instability during the freezing
56 process (Bhatnagar et al., 2008; Chang et al., 1996). Finally, the pore size of a dried product also affects the
57 reconstitution time, which is not a negligible factor to be considered, especially for highly concentrated
58 products. While low-concentration formulations generally reconstitute in less than 1 min (Lewis et al., 2010),
59 it may take up to 1 h for higher concentrated systems to yield an injectable solution (Shire et al., 2004),
60 which can be a critical issue clinically.

61 The possibility to control the nucleation temperature during freeze drying would therefore make it possible
62 to modulate the overall process efficiency, and the critical attributes of the final product as well. Moreover,
63 the batch homogeneity, which is a key requirement in the pharmaceutical and reference standard industries,
64 may be improved. It is therefore not surprising that various techniques have been developed over the years
65 to address this problem (Geidobler and Winter, 2013; Kasper, 2011; Pisano, 2019). Recent studies have
66 shown that induced nucleation has no deleterious effects and can even improve the lyophilization of model
67 proteins such as LDH (Fang et al., 2018), monoclonal antibodies (MAbs) (Awotwe-Otoo et al., 2013) and
68 human growth hormone (Oddone et al., 2020). In this study we will look at the impact of induced nucleation
69 on the reconstitution time of human plasma after freeze drying and the recovery of Factor VIII activity in that
70 plasma. Coagulation Factor VIII (FVIII:C) is the most labile haemostatic protein, whose activity is routinely
71 used to study/assess protein stability in plasma (Allain JP et al., 1983; Carlebjörk G et al., 1986; Takahashi H
72 et al., 1986; Swärd-Nilsson AM et al., 2006).

73 One commercially available solution the ice-fog technique (Brower et al., 2015; Geidobler et al., 2012;
74 Patel et al, 2009; Rambhatla et al., 2004), uses small ice particles, generated by the release of cold nitrogen
75 within the freezing chamber and that penetrate into the vials, to trigger ice nucleation. This ice fog could also
76 be generated within an external condenser, or another cold chamber. Vacuum could be established in the
77 freeze-dryer, while maintaining the condenser at atmospheric pressure. When connection is established

78 between the dryer and the condenser, the ice fog is transported into the drying chamber, inducing nucleation
79 (Ling, 2014; Umbach, 2017). Another approach, based on rapid pressurization/depressurization of the
80 drying chamber, may also be used (Bursac et al., 2009; Gasteyer et al., 2017; Konstantinidis et al., 2011).
81 However, not all freeze dryers can accommodate the overpressuring required to apply this high-pressure-
82 shift or depressurization method.

83 In this work, the so-called vacuum induced surface freezing (VISF) technique, also known as vacuum
84 induced nucleation (VIN), will be used. In VISF, a reduction in chamber pressure is used to trigger ice
85 formation in products that have been previously equilibrated at the desired nucleation temperature (T_n). The
86 nucleated samples are then held for a given amount of time (generally about 1 h) at the same or another
87 temperature (T_m) to promote the formation of large ice crystals. This results in a larger pore size, faster
88 primary drying rate, and reduced ice-water surface area compared to conventional freezing. This method
89 was first proposed by Kramer et al. (2002), and later used by other groups (Arsiccio et al., 2018; Liu et al.,
90 2005; Oddone et al., 2014; Oddone et al., 2016; Oddone et al., 2017). Representative profiles of fluid
91 temperature and chamber pressure during application of this technique are shown in Figure 1.

92 Here, the method by Oddone et al. (2014; 2016; 2017), will be applied to human plasma, a highly
93 concentrated system that is commonly freeze dried. In the context of freeze-drying, the term high-
94 concentration protein formulation is generally applied to preparations ranging from 50 to about 150 mg/ml of
95 protein (Garidel and Presser, 2019). This type of formulations typically shows increased viscosities, high
96 opalescence, phase separation or particle formation phenomena that are uncommon in low-concentration
97 preparations. Human plasma can perfectly fit into this definition, as it contains a huge amount of proteins.
98 Among them, FVIII is an essential clotting factor whose impaired function results in haemophilia A, a rare,
99 sex-linked bleeding disorder. FVIII is a labile plasma protein, which is particularly sensitive to denaturation
100 stresses. The effect of controlled nucleation on the stability of FVIII will be investigated, and a comparison
101 will be made with spontaneous freezing. This analysis will be performed both immediately after freeze drying,
102 and after 1, 3, 6 or 9 months accelerated degradation stability study at different temperatures (Kirkwood,
103 1977; Kirkwood, 1984; Kirkwood and Tydeman, 1984). The reconstitution time of the dried cakes obtained
104 after the two freezing protocols will also be assessed.

105

106 **2. MATERIALS AND METHODS**

107 **2.1 Material for filling**

108 Screened human plasma (Blood Group: A+, National Blood & Transplant, Colindale, UK) was thawed and
109 Hepes (free acid H3375, Sigma Merck, Poole, UK) was added to a final concentration of 40 mM and the bulk
110 held over ice with gentle stirring. Batches of one ml aliquots were dispensed using a Hamilton autodilutor
111 (Hamilton M510B, supplied by Microlab Technologies Ltd, Westcliff -on Sea, UK) into 5 ml ampoules (glass
112 type I, Schott supplied by Adelphi Tubes, Haywards Heath, UK) and fitted with 13mm diameter halobutyl
113 rubber lyo-closures (West Pharma, supplied by Adelphi) – partially inserted to allow sublimation to occur. A
114 batch of 100 ampoules was prepared on each of two occasions and the coefficient of variation (CV) of fill
115 assessed by measuring empty, filled and dried weights on three ampoules across the batch. The ampoules
116 were then loaded directly onto a freeze dryer (LyoBeta 15, Telstar Azbil SpA, Terrassa, Spain) and the
117 freeze drying cycle begun.

118

119 **2.2 Freeze drying cycle**

120 Two consecutive cycles were performed, one with spontaneous nucleation and one with VISF controlled
121 nucleation. During the VISF cycle, the product was first equilibrated at -5 °C for about 1 h. The pressure was
122 then reduced to a low value (about 1 mbar), promoting a strong evaporation from the ampoules, and
123 therefore a decrease in temperature that triggered nucleation. As soon as nucleation was induced in all
124 ampoules, pressure was quickly released to the atmospheric value to avoid boiling of the solution. The
125 product was then equilibrated at -10 °C for about 45 min before the final ramp to -50 °C. The combination
126 $T_n=-5^{\circ}\text{C}$, $T_m=-10^{\circ}\text{C}$ was selected based on previous observations (Oddone et al., 2016), where different
127 values for both equilibration temperatures were tested. $T_n=-5^{\circ}\text{C}$ should guarantee the formation of large ice
128 crystals. Lower temperature values (e.g, -10°C) were found to result in a smaller crystal size, while, for
129 instance, $T_n=+5^{\circ}\text{C}$ increased the within-ampoule heterogeneity. Different values of T_m were also compared
130 [Oddone et al., 2016]. It was observed than when T_m was too high, for instance equal to -5°C , the solution
131 could not freeze completely during the holding stage, and thus froze as soon as the temperature of the heat
132 transfer fluid was decreased to $-45/-50^{\circ}\text{C}$. This resulted in smaller ice crystals, and therefore larger ice-water
133 surface area, within the product. By contrast, $T_m=-10^{\circ}\text{C}$ improved the situation, promoting the formation of
134 large ice crystals during the holding step and avoiding melting back phenomena. For spontaneous freezing,
135 a continuous $0.5^{\circ}\text{C}/\text{min}$ ramp to -50°C was performed.

136 For both the spontaneous and the VISF cycle, the product was held at -50°C for 3 h to complete freezing.
137 The product was then held at -50°C for 1 h at 0.2 mbar , and for 1 h at 0.1 mbar. The temperature was
138 subsequently raised to -12°C in 1 h and held at 0.1 mbar for 30 h. Secondary drying was eventually

139 performed at 25 °C for 20 h. A 10 h ramp between primary and secondary drying was used. After the cycle
 140 the dryer was back-filled with dry nitrogen (from boil off of pure liquid nitrogen) and the closures stoppered
 141 down before ampoules were removed from the dryer. Ampoules were then flame-sealed using a manual
 142 ampoule sealer (Ampulmatic, Adelphi Tubes).

143 A scheme of the protocols used for freeze drying is shown in Table 1.

144

145 Table 1. Scheme of the experimental protocols used in this work for the freeze drying of human plasma.

146 SPON: spontaneous nucleation, VISF: vacuum induced surface freezing.

Step	SPON			VISF		
	T, °C	P, mbar	t, h	T, °C	P, mbar	t, h
Freezing						
holding	-5	-	1	-	-	-
nucleation	-5	~1	-	-	-	-
holding	-10	-	0.75	-	-	-
ramp	-50	-	1	-50	-	1.5
holding	-50	-	3	-50	-	3
SPON/VISF						
T, °C			P, mbar		t, h	
Primary Drying						
holding	-50		0.2		1	
holding	-50		0.1		1	
ramp	-12		0.1		1	
holding	-12		0.1		30	
Secondary Drying						
ramp	25		0.1		10	
holding	25		0.1		20	

147

148

149 In each batch, the temperature profile inside one ampoule was monitored by means of T-type
 150 copper/constantan miniature thermocouples placed at the bottom centre of the vial, and touching the bottom.
 151 During drying, both a capacitance (MKS Baratron) and a thermal conductivity (Pirani) manometer were used
 152 to monitor the pressure inside the drying chamber. The capacitance manometer always outputs the exact
 153 value of pressure within the chamber, while the Pirani gauge readings are shifted to higher values during
 154 primary drying. When the Pirani sensor readings begin to decay, the onset time is reached, indicating that a
 155 significant number of ampoules have completed the sublimation process (Patel et al., 2010). When the
 156 readings of the Pirani and Baratron manometers eventually converge, the offset time is reached, indicating
 157 that sublimation has ended in all the batch (see Figure 2). The offset time can be considered as the end of
 158 the primary drying phase, while the difference between offset time and onset time (in the following referred to

159 as onset-offset time) is a measure of within-batch heterogeneity. The larger this difference the greater the
160 difference in sublimation behavior of ampoules within the batch.

161

162 **2.3 FVIII assay, reconstitution times and stability study**

163 FVIII chromogenic assays, for potency determination of FVIII in ampoules prepared by the two different
164 freezing protocols, were carried out on the ACLTOP 550 analyzer (Werfen Ltd., Birchwood, UK) using the
165 Coatest SP4 FVIII chromogenic kit (Chromogenix, Werfen Ltd., Birchwood, UK), according to European
166 Pharmacopoeia guidelines (Ph. Eur. monograph Human coagulation factor VIII - 0275). Briefly, optimal
167 amounts of calcium and phospholipids, and excess amounts of factors IXa (FIXa) and X (FX) were added to
168 the reconstituted test sample containing the FVIII analyte, and under these conditions, factor X is converted
169 to FXa by FIXa, where the rate of FX activation is dependent on the amount of FVIII present in the test
170 sample. The FXa generated hydrolyses the chromogenic substrate and the amount of colour produced is
171 read photometrically at 405 nm. The intensity of colour is therefore proportional to the amount of FVIII in the
172 test sample.

173 For the stability studies, freeze dried ampoules of human plasma containing FVIII were put down for
174 storage at degradation temperatures of +45°C, +37°C, +20°C, +4°C and -20°C. Assessment of the stability
175 of the FVIII was carried out through accelerated degradation studies which allow the prediction of
176 degradation rates of samples stored at low temperatures (e.g. -20°C) based on the observed loss in potency
177 of samples stored at elevated temperatures (e.g. +4, +20, +37, +45 °C) (Kirkwood, 1977). This is an indirect
178 method used routinely to determine rate of loss based on the Arrhenius equation, where a first order reaction
179 rate is assumed (Kirkwood, 1984; Kirkwood and Tydeman, 1984).

180 Test ampoules were retrieved from different storage temperatures, at different time points and each
181 ampoule was reconstituted as described in the current European Pharmacopoeia guideline, (Ph. Eur.
182 general chapter section - assay of human coagulation factor VIII, monograph 2.7.4). Briefly, to each test
183 ampoule, 1 ml sterile water was added followed by gentle swirling and then allowed to stand at ambient
184 temperature until dissolved.

185 The time for full reconstitution was obtained for the two different freezing protocols. The reconstituted
186 samples were then assayed on the ACLTOP 550 analyser, where each sample was diluted (1/50, 1/100 &
187 1/200) in kit buffer in duplicates prior to the chromogenic assay run. Assays were carried out relative to the
188 WHO 6th International Standard (WHO 6th IS) FVIII/VWF Plasma (07/316) for potency estimation or relative
189 to pre-freeze-drying liquid sample for assessment of % loss in potency or relative to the respective -20°C

190 freeze-dried samples to assess stability. Results were analysed using CombiStats software, version 5.0
191 (1999-2013 EDQM/Council of Europe).

192

193 **2.4 Scanning electron microscopy analysis**

194 The pore dimensions of the products obtained after freeze-drying was analysed using a Scanning Electron
195 Microscope (SEM). Three samples from both the spontaneous and the VISF cycle were examined. Each
196 sample was cut along the vertical axis of the cake, and a central section was mounted onto aluminium stubs
197 with conductive silver paint (Agar Scientific, Stanstead, UK). Samples were sputter coated with 4nm gold and
198 imaged immediately after mounting. Imaging was carried out by a JSM 7401F SEM (Jeol Ltd, Welwyn
199 Garden City, UK) operating at 5kV. Images were obtained by secondary electron detection. SEM images
200 were recorded at the top, centre and bottom of each cake.

201 For analysis, approximately 50 pores were selected in each image (at x50 magnification), and each of
202 them was approximated to an ellipse. The diameter of the circle having the same area to perimeter ratio of
203 the approximating ellipse was then assumed as pore dimension, and the numerical average of the obtained
204 distribution was assumed as the average pore size, D_p , of the product.

205

206 **2.5 BET determination of specific surface area**

207 Nitrogen (N_2) adsorption method was used in a physisorption analyser (ASAP 2020 Plus, Micromeritics,
208 Norcross, GA, USA) to determine the specific surface area (SSA) of freeze dried samples. The samples
209 were degassed for 5 h at 293 K under vacuum. N_2 adsorption isotherms were acquired at 77 K in a P/P_0
210 (relative pressure) range of 0.005-0.99. For the BET analysis, 12 points in the range $P/P_0=0.05-0.30$ were
211 then used. In all cases, the sample size was between 250 and 300 mg.

212

213 **3. RESULTS**

214 **3.1 Performance of the Freezing Protocols**

215 The positive effects of VISF on primary drying time, already discussed in the literature (Arsiccio et al., 2018;
216 Oddone et al., 2014; Oddone et al., 2016), were confirmed in this work. As shown in Figure 2a, primary
217 drying lasted about 17.6 h for the spontaneous cycle (difference between offset time and the beginning of the
218 drying process). Moreover, the onset-offset time in this case amounted to about 4.2 h. In contrast, primary
219 drying was shorter, about 13.1 h, when the VISF technique was applied (Figure 2b). This result is not
220 negligible, as it corresponds to approximately 25.6 % reduction in sublimation time upon application of

221 controlled nucleation. The onset-offset time, which is a measure of variability in sublimation behaviour, also
 222 decreased to about 3 h when controlled nucleation was used. This suggests that the application of VISF is
 223 beneficial when homogeneity is an issue, and this effect may be even more significant in the case of large
 224 industrial-scale batches.

225 The observed difference in sublimation rate between spontaneous and controlled nucleation may be
 226 related to a difference in pore size. The VISF technique made it possible to induce nucleation in all samples
 227 at a high temperature (-5 °C), where formation of ice nuclei is still not observed in spontaneously-frozen
 228 ampoules. For instance, the thermocouple-containing ampoule during the spontaneous run nucleated at
 229 about -15 °C (as shown in the inset of Figure 2a). In turn, a high nucleation temperature translates into the
 230 formation of large ice crystals, that subsequently convert into equally large pores when ice is removed during
 231 sublimation. The removal of water vapour through these pores occurs with a significantly reduced resistance
 232 to mass transfer, boosting the sublimation process.

233 This hypothesis was confirmed from viewing the SEM images shown in Figure 3, where the VISF
 234 technique evidently promoted the formation of larger pores compared to spontaneous nucleation. The
 235 images for one sample only are displayed in Figure 3, but the same trend was observed for all the three
 236 ampoules analyzed, as detailed in Table 2. The use of microscopy to assess the structure of frozen or freeze
 237 dried cakes has been reported several times in the literature (Vollrath et al., 2019; Goshima et al., 2016;
 238 Abdul-Fattah et al., 2008), and here the SEM images were also quantitatively analyzed, similarly to what was
 239 done in previous works, where frequency domain image analysis (Grassini et al., 2016) or segmentation
 240 approaches (Arsiccio et al., 2019) were used for this purpose.

241

242 Table 2. Pore dimension D_p (as measured by SEM) and BET specific surface area (as measured by N_2
 243 adsorption) in the dried product, for spontaneous and controlled nucleation (average \pm standard deviation).
 244 For the BET surface area, two repetitions were made, and both sets of measurements are reported in the
 245 last column.

Sample #	Freezing Protocol	D_p , μm			BET surface area, m^2/g
		bottom	centre	top	
1	VISF	118 ± 49	130 ± 68	115 ± 71	0.19 ± 0.01 0.25 ± 0.01
2		120 ± 48	131 ± 58	115 ± 58	
3		104 ± 46	121 ± 47	107 ± 55	
1	Spon.	49 ± 15	65 ± 21	52 ± 13	0.41 ± 0.01 0.40 ± 0.01
2		51 ± 18	65 ± 18	52 ± 13	
3		68 ± 17	68 ± 15	65 ± 15	

246

247

248 Here, the difference in pore dimension was quantified by an image analysis technique, where each pore was
249 approximated to an ellipse, and the diameter of the circle having equal area to perimeter ratio was
250 computed. Averaging over all the samples, the VISF technique resulted in a dried cake with pore size in the
251 order of about 114, 127 and 112 μm at the bottom, centre and top, respectively. The presence of larger
252 pores at the centre of the cake is common during freeze-drying, because the contact with the dryer shelves,
253 and the presence of cryo-concentration effects promote the formation of a less open structure at the cake
254 edges. In contrast, the average values for the spontaneously nucleated samples were lower, about 56, 66
255 and 56 μm at the bottom, centre and top, indicating that the lower nucleation temperature in these samples
256 approximately halved the pore size compared to the case of the VISF cycle.

257 The SEM data were confirmed by the BET specific surface area (SSA) values, also listed in Table 2. As
258 expected, a larger pore size obtained when applying controlled nucleation resulted in a smaller SSA, which
259 as will be shown in the following, may have an impact on protein stability.

260

261 **3.2 FVIII residual activity**

262 In this study, as FVIII is the most labile haemostasis protein in plasma, it was decided that assessment of the
263 functional activity of FVIII in the freeze-dried samples would allow more clearly to discern any differences
264 between the 2 freeze drying techniques. The potency of FVIII was measured post-drying (n=2), and after 1
265 (n=1), 3 (n=1), 6 (n=2) or 9 (n=2) months storage at 45°C, 37°C, 20°C, 4°C or -20 °C, using the FVIII
266 chromogenic assay, as described in the methods section. The FVIII activity of the plasma sample before
267 lyophilisation was also measured relative to the WHO 6th IS and gave a value of 0.42 IU/ml [95%CL: 0.38 –
268 0.46].

269 Figure 4a illustrates FVIII potencies measured relative to the WHO 6th IS, for 6 months storage and, as
270 expected, FVIII potency decreased during storage especially at the highest temperature (37°C and 45°C).
271 Furthermore, the graph indicates a marked difference between the 2 freeze drying techniques with the VISF
272 technique showing higher potencies compared to spontaneously frozen samples. This is reflected in greater
273 % loss in potency (i.e. potencies relative to pre-freeze-drying liquid samples) for the spontaneously frozen
274 samples compared to VISF samples, see Figure 4b.

275 Furthermore, the residual FVIII potencies for ampoules stored at +4°C, +20°C, +37°C and +45°C, for the
276 two different freezing protocols, were expressed relative to ampoules stored at -20°C using an arbitrary value
277 1.00 for the -20°C ampoules. The Arrhenius model was then fitted to the data to obtain predictions of the
278 expected loss in potency over time. Figure 5 shows the Arrhenius plot (logarithm of rate vs. inverse of

279 temperature) for FVIII degradation observed during storage after spontaneous nucleation (blue) and vacuum
 280 induced surface freezing (red). The experimental points have been fitted with a line, and the R² values
 281 obtained are good, pointing towards an Arrhenius behavior. While non-Arrhenius aggregation has sometimes
 282 been observed (Wang and Roberts, 2013), the Arrhenius kinetics has often been found to be valid for
 283 lyophilized products (Wang et al., 2009; Duddu and Dal Monte, 1997; Breen et al., 2001; Perez-Moral et al.
 284 2010). Indeed in a study on behalf of the Scientific & Standardisation Committee of the International Society
 285 on Thrombosis and Haemostasis Hubbard et al demonstrated not only was the Arrhenius model a good fit
 286 for lyophilised plasma with four coagulation factor markers, but that factor VIII was the most labile of the
 287 factors studied (Hubbard et al 2010).

288 The predicted mean % loss per year, based on above data after 9 months storage at the different
 289 elevated temperatures, for the VISF technique and the spontaneous nucleation, were calculated and are
 290 shown in Table 3.

291
 292
 293
 294

Table 3. Mean predicted degradation rates expressed as % loss per year after storage for 9 months.

Chromogenic FVIII Potency Method	[§] Mean predicted % loss per year [95% upper confidence limits of predicted loss]			
	-20°C	+4°C	+20°C	+37°C
Spontaneous Nucleation	0.001 [0.001]	0.198 [0.382]	5.994 [8.598]	80.216 [80.702]
Controlled (VISF) Nucleation	0.000 [0.000]	0.003 [0.009]	0.640 [1.155]	60.951 [66.728]

295 [§]These results are based on stability data obtained from 4 time points over a 9-months period.

296

297 The predicted % loss in FVIII potency per year tended to be greater for the spontaneous nucleation
 298 compared to controlled nucleation (e.g. 0.198 vs 0.003 respectively for storage at +4°C). These results
 299 indicate a greater stability of the FVIII molecule in human plasma, when freeze dried under controlled (VISF)
 300 nucleation compared to spontaneous nucleation.

301

302 3.3 Reconstitution times

303 The reconstitution time is a crucial parameter for all pharmaceutical lyophilizates, and the freeze drying
 304 process should be designed so as to deliver a suitable reconstitution step. In this work, the reconstitution
 305 time of freeze-dried plasma was measured after storage at different temperatures for 1, 3, 6 or 9 months, in
 306 the case of both controlled and spontaneously nucleated samples. Reconstitution time of freeze-dried
 307 plasma WHO Reference Standard (07/316) was also obtained for comparison.

308 The results of this analysis are reported in Table 4 and indicate a remarkable improvement in
 309 reconstitution time when the VISF technique was applied. This is evident already for the case of storage at
 310 low temperature, where VISF approximately halved the reconstitution time. For instance, it took about 4, 5.2
 311 and 7.7 min to obtain a clear solution from the VISF samples stored for 6 months at -20 °C, 4 °C or 20 °C,
 312 respectively, while the corresponding times for conventional freezing were 11.7, 15.3 and 15.4 min. Similar
 313 improvements in reconstitution times of VISF technique were observed when compared to reconstitution
 314 times of the WHO reference standard (07/316). For samples stored at higher high temperatures (37°C or
 315 45°C), the freeze-dried bulk can harden, forming insoluble clumps and the sample can become compacted
 316 and difficult to solubilize with water. This was observed with some samples, albeit less so with the VISF
 317 technique compared to conventional freeze-drying, where reconstitution with water did not occur within 25
 318 minutes (Table 4).

319

320 Table 4. Reconstitution times (n=1) of freeze dried cakes after storage at controlled temperature.

Time months	Reconstitution Times, min										
	-20 °C storage			4 °C storage		20 °C storage		37 °C storage		45 °C storage	
	Spon.	VISF	Ref. Std	Spon.	VISF	Spon.	VISF	Spon.	VISF	Spon.	VISF
1	13.5	7.0	12.3	-	-	-	-	21 [^]	20	#	22
3	10.6	5.5	11.5	-	-	-	-	22	20	#	#
6	11.7	4.0	10.0	15.3	5.2	15.4	7.7	#	20.8 [^]	-	-
9	11.5	5.0	10.4	-	-	15.0	10.5	-	-	#	20 [^]

321 [^] Some insoluble clumps still present

322 # Did not reconstitute within 25 min

323 - Reconstitution not carried out

324

325 4. DISCUSSION

326 In previous studies, application of the depressurization technique to lactate dehydrogenase (Fang et al.,
 327 2018) reduced the degradation of LDH during the freezing process, but did not markedly improve protein

328 stability during the entire freeze-drying process. Controlled nucleation by depressurization was also reported
329 to suppress glass fogging, i.e., the undesired migration of protein solutions up on the inner walls of glass
330 vials during the freezing step of lyophilization, and to result in higher stability against shaking stress (Singh et
331 al., 2018). Application of the ice-fog technique (Vollrath et al., 2018) to lyophilized monoclonal antibody
332 formulations stored at different temperatures reduced particle formation in highly concentrated systems.
333 However, the addition of polysorbates resulted in an overall lower particle level, with no further advantage of
334 controlled nucleation on protein stability. At low concentration, no difference with respect to particle formation
335 between the controlled and spontaneously nucleated samples was detected. These results are in line with
336 our previous study (Oddone et al., 2020), where HPLC-SEC and a cell-based potency assay seemed to give
337 evidence for no dramatic difference in the behaviour of hGH at low concentration when either VISF or
338 spontaneous nucleation were used. Our results for the highly concentrated plasma system, combined with
339 previously published data reporting a negligible effect of controlled nucleation on protein stability in low
340 concentrated systems (Oddone et al., 2020; Vollrath et al., 2018), seem to suggest that the benefits of
341 controlled nucleation may depend on concentration. This result represents an interesting observation, that
342 warrants further investigation.

343 However, the results obtained for FVIII activity in this work seem to indicate a difference between the two
344 freezing protocols, with the VISF technique resulting not only in improved process efficiency, but also in
345 enhanced protein stability. This reduced loss in protein activity may be related to the smaller ice-water
346 interface resulting from application of controlled nucleation. As evident from the SEM images and the BET
347 analysis, the VISF technique promoted the formation of structures having larger ice crystals, that expose a
348 reduced surface area compared to spontaneously nucleated samples. As a result, the risk that the protein
349 adsorbs and denatures at the ice interface is reduced, likely promoting the observed preservation of the
350 native structure. It must also be borne in mind that FVIII is a much larger multi-domain protein with complex
351 intermolecular interactions which can impact on its activity, and so direct comparison to a small protein like
352 hGH (Oddone et al., 2020) may not be appropriate. An Arrhenius-based model for measuring stability was
353 used [Kirkwood 1977,1984, Kirkwood et al 1984] for convenience and comparison between the two
354 preparation are drawn. However, non-Arrhenius based models have been used by others [Jameel et al
355 2009].

356 When storage at high temperature is considered, application of the VISF technique made it possible to
357 reconstitute samples that would not return to a liquid, clump-free solution if freeze dried by conventional
358 freezing.

359 For instance, the VISF sample stored for 1 month at 45 °C could be reconstituted, while this was not
360 possible in the case of conventional freezing (see Table 4). Similarly, it was possible to reconstitute the
361 sample frozen by controlled nucleation and then stored for 6 months at 37 °C, even though some insoluble
362 clumps were still present after 25 min, while the same result could not be achieved in the case of
363 spontaneous freezing.

364 When rehydrating a freeze dried product, the gas within the pores should be displaced by the
365 reconstitution medium so as to allow wetting of the cake. Afterwards, hydration of the solid may take place. A
366 large pore size may promote the displacement of gas from the cake, and this is probably the reason for the
367 observed behaviour. This same explanation was proposed in a previous work (Geidobler et al., 2013), where
368 application of the ice-fog technique shortened the reconstitution time of highly-concentrated protein
369 formulations. A similar reduction in reconstitution time was observed when the depressurization technique
370 was applied to highly concentrated monoclonal antibody solutions (Singh et al., 2018).

371 Overall, the benefits observed when using controlled (VISF) nucleation (compared to spontaneous
372 nucleation) in the freeze drying process of plasma (i.e. increased stability and quicker reconstitution) are
373 likely to be extremely important in the development of reference plasma standards and reagents. Although in
374 this work the lyophilised plasma is a reference material and the shorter reconstitution time is therefore purely
375 a convenience, faster reconstitution of therapeutic plasma-derived products would be of enormous clinical
376 benefit, in particular in on-demand treatment.

377

378 **5. CONCLUSIONS**

379 Two different freezing protocols, with or without the possibility to control the nucleation temperature, have
380 been used to freeze dry human plasma. A degradation study has been subsequently performed, and both
381 the potency of FVIII and the reconstitution time have been measured in ampoules stored at different
382 temperatures for up to 9 months. Overall, our results suggest that the controlled nucleation approach results
383 in reduced primary drying time, because it promotes the formation of larger pores within the dried cake. The
384 difference in cake morphology between the two freezing protocols also accounts for the improvement in
385 reconstitution time in samples obtained by controlled nucleation. The easier displacement of gas from larger
386 pores allows an easier dissolution of the highly concentrated plasma lyophilizate. At the same time, the
387 smaller ice-water surface area when pores are large minimizes the risk of protein adsorption, and
388 denaturation, at the ice interface. This may be at the basis of the improvement in FVIII potency for ampoules
389 obtained by the VISF technique. Combined with previously published data, our findings suggest that the

390 benefits of controlled nucleation on protein stability may be more pronounced for highly concentrated
391 systems. This is an interesting finding and will be the subject of future investigations.

392

393 **ACKNOWLEDGEMENTS**

394 The Italian Ministry for Research and University is gratefully acknowledged for the PhD studentship to
395 Andrea Arsiccio. Chiara Vitale Brovarone, Sonia Fiorilli, Carlotta Pontremoli and Claudia Udrescu are
396 thankfully acknowledged for their help with BET analyses.

397 **REFERENCES**

- 398
399 Abdul-Fattah, A.M., Lechuga-Ballesteros, D., Kalonia, D.S., Pikal, M.J., 2008. The impact of drying method
400 and formulation on the physical properties and stability of methionyl human growth hormone in the
401 amorphous solid state. *J. Pharm. Sci.* 97, 163-184.
- 402 Allain JP, Friedli H, Morgenthaler JJ, Pflugshaupt R, Gunson HH, Lane RS, Myllylä G, Rock GA, Stryker MH,
403 Woods KR, 1983. International Forum: What are the critical factors in the production and quality
404 control of frozen plasma intended for direct transfusion or for fractionation to provide medically
405 needed labile coagulation factors. *Vox Sang.* 44, 246–259
- 406 Arsiccio, A., Barresi, A.A., De Beer, T., Oddone, I., Van Bockstal, P-J., Pisano, R., 2018. Vacuum induced
407 surface freezing as an effective method for improved inter- and intra-vial product homogeneity. *Eur.*
408 *J. Pharm. Biopharm.* 128, 210-219.
- 409 Arsiccio, A., Sparavigna, A.C., Pisano, R., Barresi, A. A., 2019. Measuring and predicting pore size
410 distribution of freeze-dried solutions. *Dry. Technol.* 37, 435-447.
- 411 Assay of human coagulation factor VIII, monograph 2.7.4. Ph. Eur. 8th edition. Strasbourg, France: Council
412 of Europe; 2014.
- 413 Awotwe-Otoo, D., Agarabi, C., Read, E.K., Lute, S., Brorson, K.A., Khan, M.A., Shah, R.B., 2013. Impact of
414 controlled ice nucleation on process performance and quality attributes of a lyophilized monoclonal
415 antibody. *Int. J. Pharm.* 450, 70-78.
- 416 Bhatnagar, B.S., Pikal, M.J., Robin, H.B., 2008. Study of the individual contributions of ice formation and
417 freeze-concentration on isothermal stability of lactate dehydrogenase during freezing. *J. Pharm. Sci.*
418 97, 798-814.
- 419 Breen, E.D., Curley, J.G., Overcashier, D.E., Hsu, C.C., Shire, S.J., 2001. Effect of moisture on the stability
420 of a lyophilized humanized monoclonal antibody formulation. *Pharm. Res.* 18, 1345-1353.
- 421 Brower, J., Lee, R., Wexler, E., Finley, S., Caldwell, M., Studer, P., 2015. New developments in controlled
422 nucleation: Commercializing VERISEQ® nucleation technology, in Varshney, D., Singh, M. (Eds.),
423 *Lyophilized Biologics and Vaccines*. Springer, New York.
- 424 Bursac, R., Sever, R., Hunek, B., 2009. A practical method for resolving the nucleation problem in
425 lyophilization. *Bioproc. Int.* 7, 6672.

426 Capozzi, L.C., Pisano, R., 2018. Looking inside the black box: Freezing engineering to ensure the quality of
427 freeze dried biopharmaceuticals. *Eur. J. Pharm. Biopharm.* 129, 58-65.

428 Carlebjörk G, Blombäck M, Pihlstedt P, 1986. Freezing of plasma and recovery of factor VIII. *Transfusion.*
429 26, 159–162.

430 Chang, B.S., Kendrick, B.S., Carpenter, J.F., 1996. Surface-induced denaturation of proteins during freezing
431 and its inhibition by surfactants. *J. Pharm. Sci.* 85, 1325-1330.

432 Council of Europe European Pharmacopoeia Commission: European Pharmacopoeia 8.2, 2014.
433 Monograph 2.7.4 Assay of human coagulation factor VIII. Strasbourg.

434 Duddu, S.P., Dal Monte, P.R., 1997. Effect of glass transition temperature on the stability of lyophilized
435 formulations containing a chimeric therapeutic monoclonal antibody. *Pharm Res.* 14, 591-595.

436 Fang, R., Tanaka, K., Mudhivarthi, V., Bogner, R.H., Pikal, M.J., 2018. Effect of controlled ice nucleation on
437 stability of lactate dehydrogenase during freeze-drying. *J. Pharm. Sci.* 107, 824-830.

438 Fissore, D., Pisano, R., Barresi, A., 2019. Freeze drying of pharmaceutical products. CRC Press, Boca
439 Raton, Florida, USA. pp. 1-192.

440 Franks, F., 1995. Protein destabilization at low temperatures. *Adv. Protein Chem.* 46, 105-139.

441 Franks, F., Auffret, T., 2009. Freeze drying of pharmaceuticals and biopharmaceuticals: Principles and
442 practice. RSC publishing, Cambridge, UK, pp. 1-206.

443 Garidel, P., Presser, I., 2019. Lyophilization of high-concentration protein formulations, in Ward, K.,
444 Matejtschuk, P. (Eds.), *Lyophilization of Pharmaceuticals and Biologicals. Methods in Pharmacology*
445 *and Toxicology.* Humana Press, New York.

446 Gasteyer, T.H., Sever, R.R., Hunek, B., Grinter, N., Verdone, M.L., May 2017. Lyophilization system and
447 method. US Patent 9651305 B2.

448 Geidobler, R., Mannschedel, S., Winter, G., 2012. A new approach to achieve controlled ice nucleation of
449 supercooled solutions during the freezing step in freeze drying. *J. Pharm. Sci.* 101, 4409-4413.

450 Geidobler, R., Winter, G., 2013. Controlled ice nucleation in the field of freeze drying: Fundamentals and
451 technology review. *Eur. J. Pharm. Biopharm.* 85, 214-222.

452 Geidobler, R., Konrad, I., Winter, G., 2013. Can controlled ice nucleation improve freeze drying of highly-
453 concentrated protein formulations? *J. Pharm. Sci.* 102, 3915-3919.

454 Goshima, H., Do, G., Nakagawa, K., 2016. Impact of ice morphology on design space of pharmaceutical
455 freeze-drying. *J. Pharm. Sci.* 105, 1920-1933.

456 Grassini, S., Pisano, R., Barresi, A.A, Angelini, E., Parvis, M., 2016. Frequency domain image analysis for
457 the characterization of porous products. *Measurement* 94, 515-522.

458 Hottot, A., Vessot, S., Andrieu, J., 2007. Freeze drying of pharmaceuticals in vials: Influence of freezing
459 protocol and sample configuration on ice morphology and freeze-dried cake texture. *Chem. Eng.*
460 *Process.* 46, 666-674.

461 Hubbard, A.R. Kitchen, S., Beeharry, M., Bevan, S.A., Bowyer, A. 2011. Long term stability of the Scientific
462 and Standardisation Committee Secondary Coagulation Standard (SSC Lot no 3) . *J Thromb.*
463 *Haemost.* 9; 1246-8.

464 Human coagulation factor VIII, monograph 0275. Ph. Eur. 8th Edition. Strasbourg, France: Council of
465 Europe; 2014.

466 Jameel F, Tchessalov S, Bjornsen E, Lu X, Bersman M, Pikal MJ. Development of a freeze dried
467 biosynthetic Factor VIII: I. A case study in the optimization of formulation. *Pharm Dev Technol*
468 2009;14:687-97.

469 Kasper, J.C., Friess, W.F., 2011. The freezing step in lyophilization: Physico-chemical fundamentals,
470 freezing methods and consequences on process performance and quality attributes of
471 biopharmaceuticals. *Eur. J. Pharm. Biopharm.* 78, 248-263.

472 Kirkwood, T.B.L., 1977. Predicting the stability of biological standards and products. *Biometrics* 33, 736-742.

473 Kirkwood, T.B.L., 1984. Design and analysis of accelerated degradation tests for the stability of biological
474 standards III. Principles of design. *J. Biol. Stand.* 12, 215-224.

475 Kirkwood, T.B.L., Tydeman, M.S., 1984. Design and analysis of accelerated degradation tests for the
476 stability of biological standards II. A flexible computer program for data analysis. *J. Biol. Stand.* 12,
477 207-214.

478 Konstantinidis, A.K., Kuu, W., Otten, L., Nail, S.L, Sever, R.R., 2011. Controlled nucleation in freeze drying:
479 Effects on pore size in the dried product layer, mass transfer resistance, and primary drying rate. *J.*
480 *Pharm. Sci.* 100, 3453-3470.

481 Kramer, M., Sennhenn, B., Lee, G., 2002. Freeze drying using vacuum-induced surface freezing. *J. Pharm.*
482 *Sci.* 91, 433-443.

483 Lewis, L., Johnson, R.E., Oldroyd, M.E., Ahmed, S.S., Joseph, L., Saracovan, I., Sinha, S., 2010.
484 Characterizing the freeze drying behavior of model protein formulations. *AAPS PharmSciTech* 11,
485 1580-1590.

486 Ling, W. Controlled Nucleation During Freezing Step of Freeze Drying Cycle Using Pressure Differential Ice
487 Fog Distribution. Patent US 8839528 B2, September 23, 2014. Patent EP 2702342 B1, April 20,
488 2014.

489 Liu, J., Viverette, T., Virgin, M., Anderson, M., Paresh, D., 2005. A study of the impact of freezing on the
490 lyophilization of a concentrated formulation with a high fill depth. *Pharm. Dev. Technol.* 10, 261-272.

491 Oddone, I., Pisano, R., Bullich, R., Stewart, P., 2014. Vacuum-induced nucleation as a method for freeze-
492 drying cycle optimization. *Ind. Eng. Chem. Res.* 53, 18236-18244.

493 Oddone, I., Van Bockstal, P-J., De Beer, T., Pisano, R., 2016. Impact of vacuum-induced surface freezing on
494 inter- and intra-vial heterogeneity. *Eur. J. Pharm. Biopharm.* 103, 167-178.

495 Oddone, I., Barresi, A.A., Pisano, R., 2017. Influence of controlled ice nucleation on the freeze drying of
496 pharmaceutical products: The secondary drying step. *Int. J. Pharm.* 524, 134-140.

497 Oddone, I., Arsiccio, A., Duru, C., Malik, K., Ferguson, J., Pisano, R., Matejtschuk, P., 2020. Vacuum
498 induced surface freezing for the freeze drying of the human growth hormone: How does nucleation
499 control affect protein stability? *J. Pharm. Sci.* [109, 254-263](#).

500 Patel, S., Bhugra, C., Pikal, M., 2009. Reduced pressure ice fog technique for controlled ice nucleation
501 during freeze drying. *AAPS PharmSciTech* 10, 1406-1411.

502 Patel, S.M., Takayuki, D., Pikal, M.J., 2010. Determination of end point of primary drying in freeze drying
503 process control. *AAPS PharmSciTech* 11, 73-84.

504 Pérez-Moral, N., Adnet, C., Noel, T.R., Parker, R. 2010. Characterization of the rate of thermally-induced
505 aggregation of β -lactoglobulin and its trehalose mixtures in the glass state. *Biomacromolecules* 11,
506 2985-2992.

507 Pikal, M.J., Rambhatla, S., Ramot, R., 2002. The impact of the freezing stage in lyophilization: Effects of the
508 ice nucleation temperature on process design and product quality. *Am. Pharm. Rev.* 5, 48-53.

509 Pisano, R., 2019. Alternative methods of controlling nucleation in freeze drying, in Ward, K., Matejtschuk, P.
510 (Eds.), *Lyophilization of Pharmaceuticals and Biologicals. Methods in Pharmacology and Toxicology.*
511 Humana Press, New York.

512 Privalov, P.L., 1990. Cold denaturation of proteins. *Crit. Rev. Biochem. Mol. Biol.* 25, 281-305.

513 Rambhatla, S., Ramot, R., Bhugra, C., Pikal, M.J., 2004. Heat and mass transfer scale-up issues during
514 freeze drying, Part 2: Control and characterization of the degree of supercooling. *AAPS*

515 PharmSciTech 5, e58.

516 Rey, L., May, J.C., 2010. Freeze drying/lyophilization of pharmaceutical and biological products, 3rd edition.
517 Informa Healthcare, London, UK, pp. 1-564.

518

519 Searles, J., Carpenter, J., Randolph, T., 2001. The ice nucleation temperature determines the primary drying
520 rate of lyophilization for samples frozen on a temperature-controlled shelf. *J. Pharm. Sci.* 90, 860-871.

521 Shire, S.J., Shahrokh, Z., Liu, J., 2004. Challenges in the development of high protein concentration
522 formulations. *J. Pharm. Sci.* 93, 1390-1402.

523 Singh, S.N., Kumar, S., Bondar, V., Wang, N., Forcino, R., Colandene, J., Nesta, D., 2018. Unexplored
524 benefits of controlled ice nucleation: Lyophilization of a highly concentrated monoclonal antibody
525 solution. *Int. J. Pharm.* 552, 171-179.

526 Strambini, G.B., Gabellieri, E., 1996. Proteins in frozen solutions: Evidence of ice-induced partial unfolding.
527 *Biophys. J.* 70, 971-976.

528 Swärd-Nilsson, A.M., Persson, P.O., Johnson, U., Lethagen, S., 2006. Factors influencing factor VIII activity
529 in frozen plasma. *Vox Sang.* 90, 33–39.

530 Takahashi H, Hanano M, Tatewaki W, Shibata A., 1986. Factor VIII lability, protein C and other vitamin K-
531 dependent proteins. *Thromb Res.* 43(5), 561-8.

532 Umbach, M. Freeze Drying Plant. Patent EP 3093597 B1, December 27, 2017.

533 Vollrath, I., Friess, W., Freitag, A., Hawe, A., Winter, G., 2018. Does controlled nucleation impact the
534 properties and stability of lyophilized monoclonal antibody formulations? *Eur. J. Pharm. Biopharm.*
535 129, 134-144.

536 Vollrath, I., Friess, W., Freitag, A., Hawe, A., Winter, G., 2019. Comparison of ice fog methods and
537 monitoring of controlled nucleation success after freeze-drying. *Int. J. Pharm.* 558, 18-28.

538 Wang, W., Roberts, C.J., 2013. Non-Arrhenius protein aggregation. *AAPS J.* 15, 840-851.

539 Wang, B., Tchessalov, S., Cicerone, M.T., Warne, N.W., Pikal, M.J. 2009. Impact of sucrose level on storage
540 stability of proteins in freeze-dried solids: II. Correlation of aggregation rate with protein structure and
541 molecular mobility. *J Pharm Sci.* 98, 3145-3166.

542 Ward, K., Matejtschuk, P., 2019. Lyophilization of pharmaceuticals and biological: New technologies and
543 approaches. *Methods in Pharmacology and Toxicology.* Humana Press, New York, pp. 1-382.

544

545 **LIST OF FIGURES**

546

547 Figure 1: Representative profiles of fluid temperature and chamber pressure during application of the VISF
548 protocol. The sample is first equilibrated at T_n , and nucleation is then induced by lowering the pressure to a
549 formulation-specific value. A second holding stage at T_m is subsequently performed to promote the growth of
550 large ice crystals.

551

552 Figure 2: Temperature and pressure profiles during a) the spontaneous run and b) the VISF run for the
553 plasma batch. Black line: fluid temperature, Red line: Product temperature, Green line: capacitance
554 manometer, Blue line: Pirani manometer. In panel a, an enlargement of the product temperature during
555 freezing is shown in the inset.

556

557 Figure 3: SEM images of the samples obtained after spontaneous (top) and controlled (bottom) nucleation.
558 The magnification is the same for all images, and the white bar in the figure corresponds to a distance of 100
559 μm .

560

561 Figure 4: (a) FVIII potency (IU/ml) measured relative to the WHO 6th IS FVIII/VWF Plasma (07/316) after 6
562 months storage at different accelerated degradation temperatures, for samples freeze dried with
563 spontaneous (open circles) or controlled VISF (filled circles) nucleation. (b) Percentage (%) loss in FVIII
564 potency post freeze-dried samples (i.e. relative to pre-freeze-drying liquid samples) with spontaneous (open
565 circles) or controlled (filled circles) nucleation, after 6 months storage at different accelerated degradation
566 temperatures. The error bars displayed in the figure correspond to standard deviation.

567

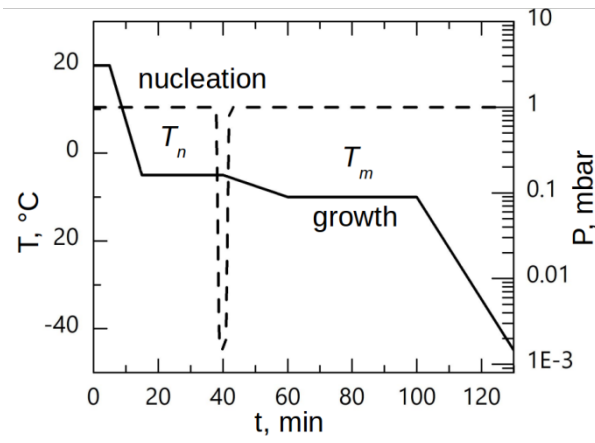
568 Figure 5: Arrhenius plot (logarithm of rate $\ln k$ vs. inverse of temperature $1/T$) for FVIII degradation observed
569 during storage after spontaneous nucleation (blue) and vacuum induced surface freezing (red). The
570 experimental points, represented as blue squares or red triangles, have been fitted with a line. The equation
571 and R^2 value of the fitting are also displayed on the graph.

572

573

574

575



576
577
578

Figure 1

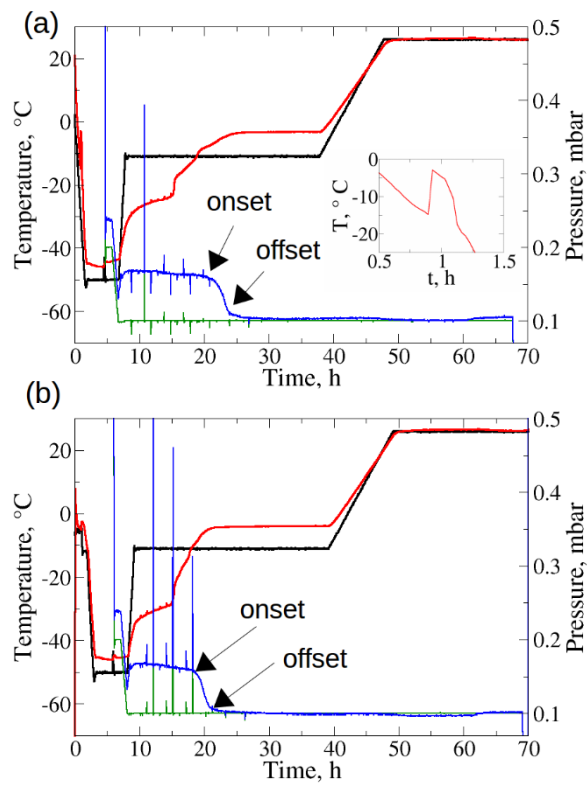
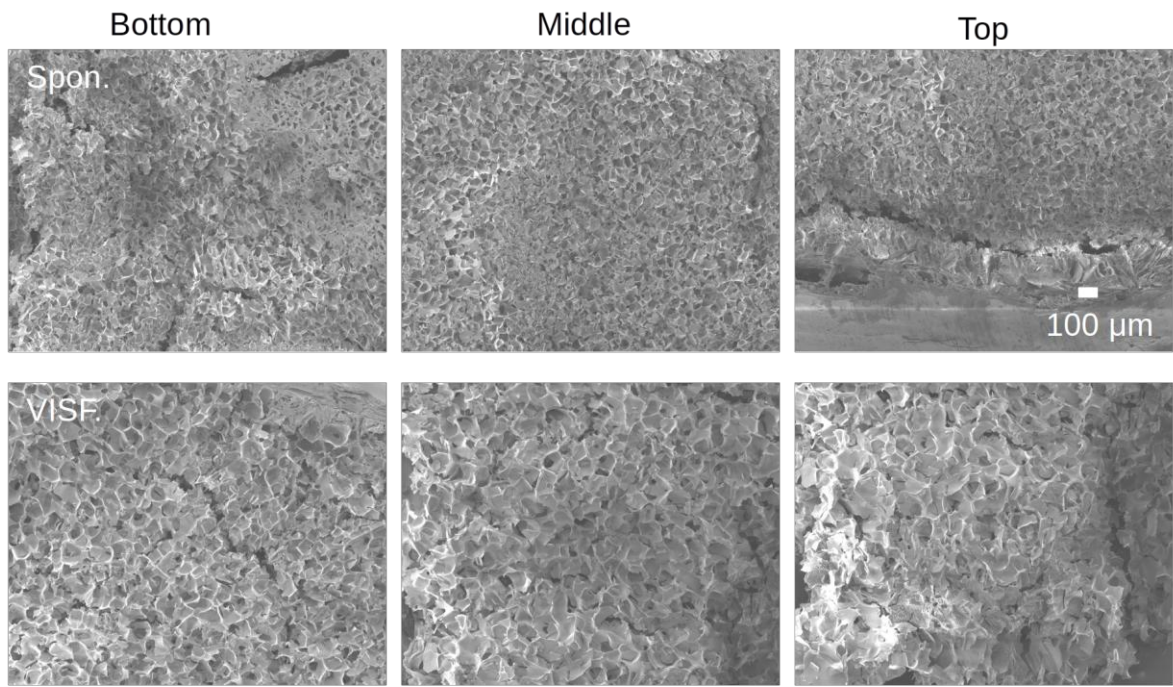


Figure 2

579
580
581
582
583
584

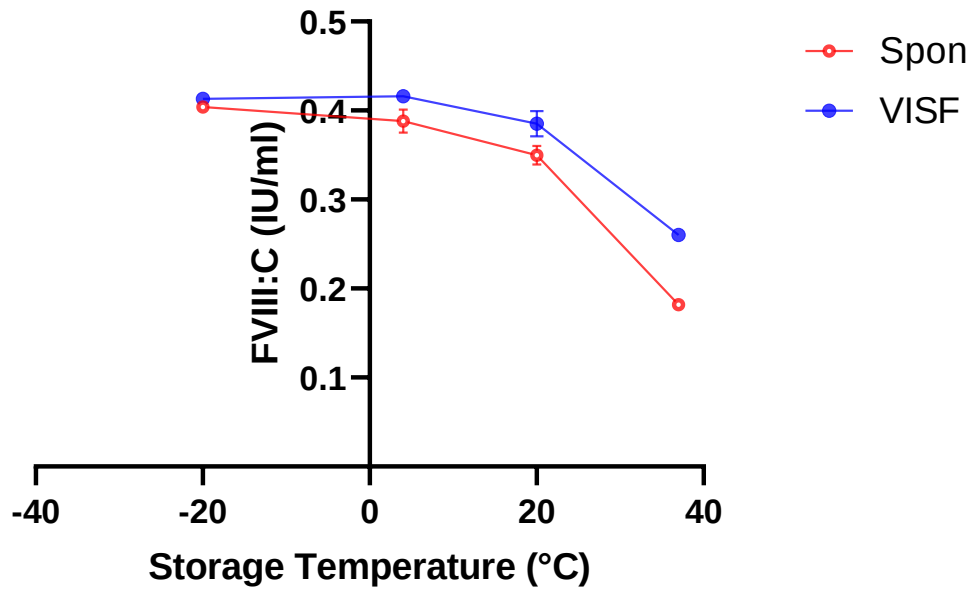
585
586
587
588
589



590
591
592
593
594
595
596
597
598
599
600
601
602
603
604
605
606
607
608
609
610
611
612

Figure 3

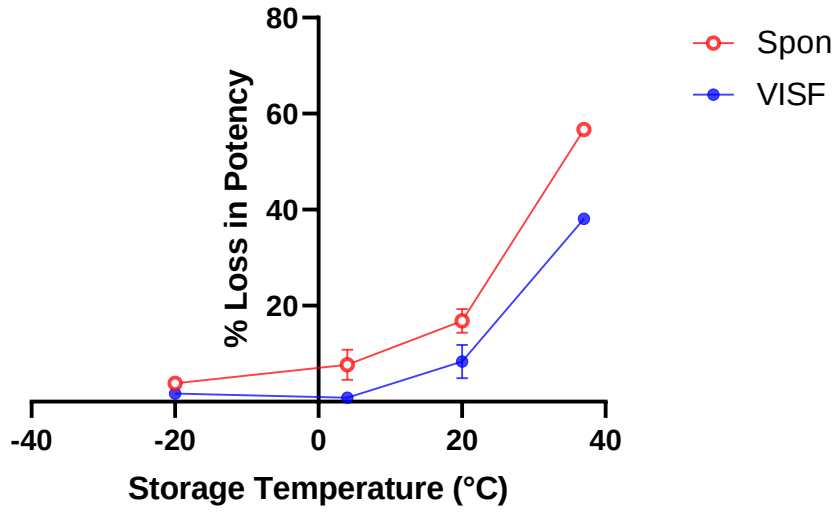
(a)



613

614
615
616

617
(b)
620



621
622
623
624
625
626

Figure 4

627
628
629

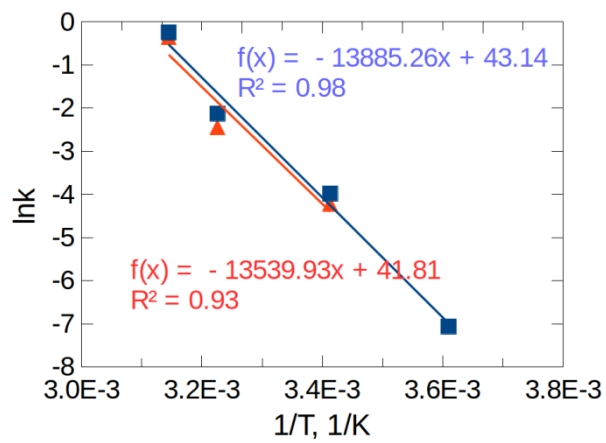


Figure 5

630
631
632
633

Declaration of interests

The authors declare that they have no known competing financial interests or personal relationships that could have appeared to influence the work reported in this paper.

The authors declare the following financial interests/personal relationships which may be considered as potential competing interests:



Paul Matejtschuk on behalf of the authorship

Credit Author Statement

We encourage you to submit an author statement file outlining all authors' individual contributions, using the relevant CRediT roles: Conceptualization; Data curation; Formal analysis; Funding acquisition; Investigation; Methodology; Project administration; Resources; Software; Supervision; Validation; Visualization; Roles/Writing - original draft; Writing - review & editing. Please format with author name first followed by the CRediT roles: for an example and more details see authorship of a paper section [here](#)

Impact of Controlled Vacuum Induced Surface

Freezing on the Freeze Drying of Human Plasma

by

Andrea Arsiccio¹, Paul Matejtschuk², Ernest Ezeajughi², Andrew Riches-Duit⁴,

Anwen Bullen^{3,5}, Kiran Malik², Sanj Raut⁴ & Roberto Pisano¹.

Credit Author Statement:

AA, PM, SR and RP all contributed to conceptualization, ARD, AB, KM and EE contributed with AA to the Investigation and Formal Analysis. AA provided the initial manuscript draft and all authors contributed to editing/revision.

Highlights

- Vacuum induced nucleation is applied to the freeze-drying of human plasma
- Cycle time is reduced and batch homogeneity improved by controlled nucleation
- Controlled nucleation enhances Factor VIII stability during degradation studies
- The application of controlled nucleation reduces the reconstitution time of the freeze dried material